Measurement of nonlinear observables in the Large Hadron Collider using kicked beams

E. H. Maclean[*]

CERN, Geneva CH-1211, Switzerland; John Adams Institute, University of Oxford,
Oxford OX1 3RH, United Kingdom;
and Cockcroft Institute, University of Manchester, Manchester M13 9PL, United Kingdom

R. Tomás, F. Schmidt, and T. H. B. Persson

CERN, Geneva CH-1211, Switzerland

The nonlinear dynamics of a circular accelerator such as the Large Hadron Collider (LHC) may significantly impact its performance. As the LHC progresses to more challenging regimes of operation it is to be expected that the nonlinear single particle dynamics in the transverse planes will play an increasing role in limiting the reach of the accelerator. As such it is vital that the nonlinear sources are well understood. The nonlinear fields of a circular accelerator may be probed through measurement of the amplitude detuning: the variation of tune with single particle emittance. This quantity may be assessed experimentally by exciting the beam to large amplitudes with kicks, and obtaining the tunes and actions from turn-by-turn data at Beam Position Monitors. The large amplitude excitations inherent to such a measurement also facilitate measurement of the dynamic aperture from an analysis of beam losses following the kicks. In 2012 these measurements were performed on the LHC Beam 2 at injection energy (450 GeV) with the nominal magnetic configuration. Nonlinear coupling was also observed. A second set of measurements were performed following the application of corrections for b_4 and b_5 errors. Analysis of the experimental results, and a comparison to simulation are presented herein.

I. INTRODUCTION

Since commissioning of the LHC began in 2009 great progress has been achieved in the measurement, correction and modeling of the linear optics [1–5]. It has also been demonstrated that the chromatic beta-beating and the chromatic coupling are extremely well understood [5,6]. In order to optimize the future performance of the machine as it moves into more challenging operational regimes however, further understanding of nonlinearities in the LHC will be essential.

Nonlinearities in the machine contribute to the dynamic aperture (DA), lead to the development of resonances in the motion, and may drive particles towards such resonant frequencies. These effects are detrimental to beam lifetime and luminosity production, and may inhibit the LHC's mission. On the other hand the introduction of well understood and controlled nonlinearity can be vital for the damping of dangerous instabilities in beam motion. To effectively control and correct the nonlinearity in operation

it is necessary to quantify the machine nonlinearity through beam-based measurements of properties determined by higher order fields. Such studies allow for verification or invalidation of the magnetic model, and are also important for the study of upgrade scenarios.

Beam based studies of nonlinearities in the LHC were first performed on LHC Beam 2 at injection energy (450 GeV) in 2011 [7–9]. It was observed that, with Landau octupoles depowered, the measured second order chromaticity and first order amplitude detuning were significantly higher than expected from the available knowledge of the magnetic errors and alignments. A substantial proportion of the discrepancy in the model was explained by hysteresis errors in the octupolar spool pieces (MCO), intended for compensation of b_4 errors in the arcs, however a significant deficit remained in the model. Correction of the second and third order chromaticities was demonstrated, and led to corresponding reductions in the amplitude detuning and the decoherence of kicked beams [8,9].

In June 2012 a new set of amplitude detuning measurements were performed on the LHC Beam 2 with the nominal magnetic configuration at 450 GeV. This included Landau octupoles (MO) powered at their operational settings (operational settings for June 2012, later in the year the MO polarity in operation was reversed).

[*]ewen.hamish.maclean@cern.ch

The crossing and separation bumps in the insertion regions were also set to their nominal values at injection: 170 μrad and ± 2 mm, respectively. Upgrades to the LHC kicker magnets, and more favorable collimation settings allowed for a substantially higher amplitude reach than in 2011. This facilitated the measurement of amplitude detuning terms higher than first order, an observation of the dynamic aperture of the LHC, and observations of the nonlinear coupling. This paper will present the results of measurements performed in 2012 along with comparisons to simulation. A CERN internal note has been produced describing these studies [10]. Nonlinear dynamics studies have also been performed on LHC Beam 1 in 2011 and 2012 using a differing methodology, descriptions may be found in [7,11,12].

The paper begins by summarizing in Sec. II the methods used to measure nonlinear beam properties in the LHC, Sec. III then provides details of the LHC model used for comparison with the measured data. Section IV begins with a general summary of the experimental procedure (Sec. IV A), then in Sec. IV B presents the results of the measurements performed together with a comparison to simulation. Four properties of the LHC are discussed: the decoherence of kicked beams, detuning with amplitude, nonlinear coupling, and the dynamic aperture.

II. MEASUREMENT OF NONLINEAR OBSERVABLES

A. Amplitude detuning

Amplitude detuning is the variation of tune with single particle emittance. This detuning may be described by a Taylor expansion about the unperturbed tune, Eq. (1).

$$Q_z(\epsilon_x, \epsilon_y) = Q_{z0} + \frac{\partial Q_z}{\partial \epsilon_x}\epsilon_x + \frac{\partial Q_z}{\partial \epsilon_y}\epsilon_y$$
$$+ \frac{1}{2!}\left(\frac{\partial^2 Q_z}{\partial \epsilon_x^2}\epsilon_x^2 + 2\frac{\partial^2 Q_z}{\partial \epsilon_x \partial \epsilon_y}\epsilon_x\epsilon_y + \frac{\partial^2 Q_z}{\partial \epsilon_y^2}\epsilon_y^2\right) + \cdots$$
(1)

$\epsilon_{x,y}$ is the physical single particle emittance. The physical single particle emittance is related to the action ($J_{x,y}$) by Eq. (2).

$$2J_{x,y} = \epsilon_{x,y}.$$
(2)

For practical purposes it may be more convenient to relate the single particle emittance to an amplitude in terms of the number of beam sigmas (σ). Assuming a Gaussian beam distribution this is given by Eq. (3).

$$N_\sigma = \sqrt{\frac{2J}{\epsilon_{\text{Beam}}}}.$$
(3)

ϵ_{Beam} is the physical emittance of the beam, which may be determined from wire scanner (*BWS*) data [13]. The nominal physical emittance of the beam at 450 GeV is 0.0078 μm (corresponding to the nominal normalized emittance of 3.75 μm), σ_{nominal} is defined as the amplitude corresponding to this emittance.

Detuning with amplitude is generated by nonlinear magnetic fields. The relevant sources for the detuning are given in Table I.

The detuning with amplitude can be measured by exciting the beam to large amplitudes using a kicker magnet. The LHC Aperture Kicker (MKA) [15–17] used in these studies is capable of providing single kicks of up to $14\sigma_{\text{nominal}}$. On applying such a kick betatron oscillations of the beam are excited. Spectral analysis of the turn-by-turn (TbT) data in the beam position monitors (BPM) then yields the tune. In these studies spectral analysis was performed using the SUSSIX code for frequency analysis of nonlinear betatron motion [18]. Performing such an analysis for a range of kick strengths allows for a measurement of the variation of tune with betatron oscillation amplitude. The mean and standard deviation obtained by performing this analysis for all BPMs (there are ~500 dual plane BPMs per beam in the LHC) are taken as the value and uncertainty on the tune.

The action of the kick may be determined from the TbT BPM data using Eq. (4)

$$2J_{x,y} = \frac{\sum_{\text{BPMs}} \frac{(\frac{1}{2}\text{Peak-to-Peak})^2}{\beta_{x,y}}}{N}$$
(4)

where Peak-to-Peak is the peak-to-peak amplitude of the turn-by-turn oscillation data in the relevant plane of the BPM and N is the number of BPMs. The procedure of averaging over the available BPMs ≈500 dual plane BPMs are available in the LHC automatically cancels the effect of first order focusing errors around the ring. The effect of the measured beta-beat on the action determined with Eq. (4) has been examined for the studies presented in this paper, and found to be negligible [19]. This reflects the high quality of the linear optics correction in the LHC.

Equation (4) makes the implicit assumption of an elliptical phase space trajectory: it is valid in the linear regime where the phase space has not been distorted by

TABLE I. Sources of detuning with amplitude [14]. In this notation K_2 represents a quadrupole. $(K_a)^b$ represents the *b*th order contribution of multipole K_a.

Order	Source
Q_0	K_2
$\frac{\partial Q}{\partial \epsilon}$	$(K_3)^2$, K_4
$\frac{\partial^2 Q}{\partial \epsilon^2}$	$(K_3)^4$, $(K_3)^2 K_4$, $(K_4)^2$, $K_3 K_5$, K_6

higher order resonances. The application of Eq. (4) to the real LHC is therefore an approximation, the validity of which will depend on the degree to which the phase space is distorted. If detuning with amplitude drives the tunes toward resonant frequencies, such distortions could impact upon the determination of the detuning. The validity of Eq. (4) under the conditions relevant to the studies presented in this paper is discussed briefly toward the end of Sec. IV B 2. This method of determining the action of the kicks also assumes that any emittance exchange due to coupling is negligible.

In the LHC corrections for various geometric and electrical nonlinearities are automatically performed on the turn-by-turn BPM data at its point of delivery to users, however there are known to be small imperfections in the compensation of the BPM nonlinearity at very large amplitudes. The correction of the BPM nonlinearity is reviewed in [20,21]. The effect of rotational alignment errors on the LHC BPM data is negligible, particularly given the procedure of averaging over the available BPMs. Prior to analysis of the turn-by-turn BPM data, singular value decomposition (SVD) cleaning was performed on a matrix constructed from the TbT data of all available BPMs [22]. This assists in the removal of uncorrelated noise.

Ideally, detuning terms in Eq. (1) are reconstructed by kicking at a range of amplitudes along several angles in the $(2J_x, 2J_y)$ plane. A fit may then be performed to the surface defined by these measurements. In practice such a procedure requires a significant amount of dedicated beam time in the LHC. Consequently measurements may be performed only in the horizontal and vertical planes. Under such conditions, when the excitation of a single plane dominates, the 2D Taylor expansion of Eq. (1) may be approximated to 1D Taylor series, Eq. (5).

$$Q_x(\epsilon_x, 0)$$
$$Q_x(0, \epsilon_y)$$
$$Q_y(\epsilon_x, 0)$$
$$Q_y(0, \epsilon_y) \qquad (5)$$

Typically it is required to perform a small excitation in the opposite plane from the dominant kick. This ensures the amplitude of the spectral line corresponding to the tune of the unkicked plane is sufficiently above the noise level to allow for a reliable determination of both tunes. So long as any variation in the excitation amplitude of this additional kick is small with respect to the amplitude range being examined, determination of the detuning is unaffected (though the effect may show up as changes in the Q_{z0} of fits to the measured data). Keeping all kicks in the subdominant plane at constant amplitude throughout the study should help ensure this condition is satisfied, however any substantial coupling of the kicks into the opposite plane will introduce complications if a 1D analysis is attempted.

Diagonal terms in the 2D Taylor expansions for Q_x and Q_y cannot be measured directly if only horizontal or vertical kicks are performed. Some of these missing terms may be determined from the well-known identities relating the diagonal terms of Q_x to the on axis terms of Q_y and vice versa. Equation (6) is the well-known equivalence of first order amplitude detuning cross terms, Eqs. (7) are the equivalent identities for the second order detuning which relate the diagonal detuning of $Q_{x,y}$ to the on axis detuning of $Q_{y,x}$.

$$\frac{\partial Q_x}{\partial \epsilon_y} = \frac{\partial Q_y}{\partial \epsilon_x} \qquad (6)$$

$$\frac{\partial^2 Q_x}{\partial \epsilon_x \partial \epsilon_y} = \frac{\partial^2 Q_y}{\partial \epsilon_x^2}$$
$$\frac{\partial^2 Q_y}{\partial \epsilon_x \partial \epsilon_y} = \frac{\partial^2 Q_x}{\partial \epsilon_y^2} \qquad (7)$$

If the data is available such identities relating the detunings of Q_x and Q_y can provide a qualitative test of the measurement quality and the fits to the data. Identities (6) relating the first order detuning cross terms allow for such a test with both 1D and 2D methods. While poor agreement of these terms in the detuning expansion may be indicative of a poor quality fit or bad data, a good agreement does not necessarily imply the reverse.

Recent theoretical advances, verified experimentally in the LHC, now allow for the study of amplitude detuning using an AC dipole kicker magnet [23]. As opposed to measurements with a single kick this has the advantage of being nondestructive, however the analysis is substantially complicated with respect to the single kick method and data quality may be lower. At injection energy in the LHC the single kick method is most suitable, and was utilized in the studies present herein. At top energy however, measurement of amplitude detuning with the AC dipole is the only feasible solution as measurement with the MKA requires the injection of fresh beam following every excitation, which is impractical at top energy within the time scales available for beam-dynamics studies.

B. Nonlinear chromaticity

Chromaticity is the variation of tune with the relative deviation from the ideal momentum (p_0). Under the influence of chromatic aberrations the tune may be described as a Taylor series about the unperturbed tune, Eq. (8).

$$Q_z\left(\frac{\Delta p}{p_0}\right) = Q_{z0} + Q_z'\left(\frac{\Delta p}{p_0}\right)$$
$$+ \frac{1}{2!}Q_z''\left(\frac{\Delta p}{p_0}\right)^2 + \frac{1}{3!}Q_z'''\left(\frac{\Delta p}{p_0}\right)^3 + \cdots, \quad (8)$$

where

$$Q_z^n = \frac{\partial^n Q_z}{\partial \frac{\Delta p^n}{p_0}} \qquad z = x, y. \tag{9}$$

Q' is the first order variation of the tune with the relative momentum deviation, and is normally referred to as the chromaticity. Q'', Q''', and further higher order terms in the Taylor expansion are referred to as the nonlinear chromaticity. Chromaticity is, in the first instance, introduced into an accelerator via the momentum dependent focusing generated by quadrupoles (higher momentum particles are less strongly focused by quadrupolar fields), thus all alternating gradient machines have substantial *natural chromaticities* which are negative. Nonlinear magnetic fields in dispersive regions also generate chromatic perturbations, thus sextupoles are commonly used to correct the natural chromaticity. The relevant sources for chromatic perturbations are given in Table II.

The chromaticity may be measured directly by observing the tune shift while varying the momentum of the beam. A change in momentum is generated via a change in the frequency of the RF-cavities. The relative momentum offset is related to the frequency shift by Eq. (10) [24], where α_C is the momentum compaction factor.

$$\frac{\Delta p}{p_0} = -\frac{1}{\alpha_C - \gamma_{\text{rel}}^{-2}} \frac{\Delta f_{\text{RF}}}{f_{\text{RF}}} \approx -\frac{1}{\alpha_C} \frac{\Delta f_{\text{RF}}}{f_{\text{RF}}}. \tag{10}$$

The variation of the momentum compaction factor with momentum in the LHC is negligible and the nonlinear chromaticity is in general calculated assuming a constant momentum compaction factor. The LHC tunes may be monitored throughout a scan of the relative momentum offset using the band based tune (BBQ) system [25].

Consulting Table II, the Q'' and Q''' may be corrected using octupole and decapole magnets, respectively, as these elements have an impact linear in their strength and will not affect the lower orders except through feed-down. The measurement and correction of second and third order chromaticity in the LHC was demonstrated in 2011, and is shown in Fig. 1. Q'' and Q''' were corrected using global trims of the octupole (MCO) and decapole (MCD) correctors in the LHC arcs. Upon correction of the second and
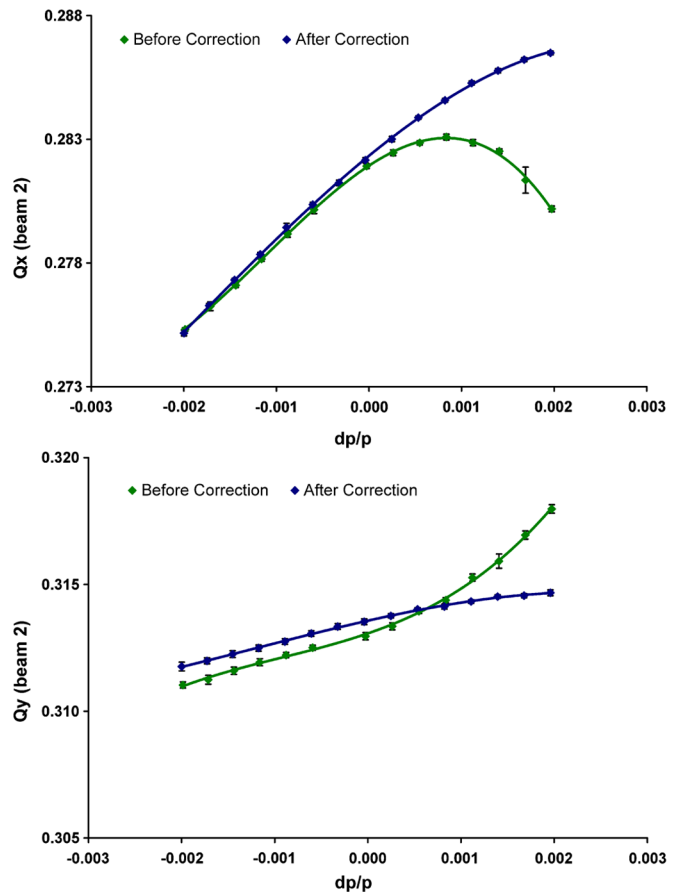

FIG. 1. Measurement of nonlinear chromaticity in the horizontal (top) and vertical (bottom) planes of the LHC at 450 GeV in 2011, before and after correction with octupolar and decapolar correctors [7,8].

third order chromaticities, reductions were observed in the first order detuning with amplitude and the decoherence of kicked beams [8,9]. It should be noted that nonlocal correction of nonlinear chromaticity does not automatically guarantee correction of the detuning with amplitude and decoherence. The observed reduction in the decoherence of kicked beams and of detuning with amplitude, upon correction of nonlinear chromaticity, reflects the fact that the corrector magnets used for the compensation are mounted directly on every second main dipole in the LHC arcs, and the main dipoles are the dominant sources of the relevant nonlinearities at injection when the Landau octupoles are unpowered. This local nature of the correction allows for the simultaneous correction of nonlinear chromaticity together with amplitude detuning and decoherence.

Measurement of the nonlinear chromaticity was not possible during the 2012 experimental period described in this paper. Trims of the RF-frequency affect both LHC beams, and would have interfered with a parallel study performed on Beam 1. The corrections for Q'' and Q''' determined in 2011 and shown in Fig. 1 were, however,

TABLE II. Sources of chromaticity [14]. In this notation K_2 represents a quadrupole. $(K_a)^b$ represents the bth order contribution of multipole K_a.

Order	Source
Q_0	K_2
Q'	K_2, K_3
Q''	$K_2, K_3, (K_3)^2, K_4$
Q'''	$K_2, K_3, (K_3)^2, K_4, (K_3)^3, K_3 K_4, K_5$

utilized in the 2012 studies presented in this paper, with the exception that the octupole trim was rescaled in order to compensate for a malfunctioning MCO family.

C. Decoherence

Beam position monitors (BPMs) record the center of charge of the beam. Amplitude detuning and chromaticity cause a tune spread in the beam. As a result, the betatron oscillations of individual particles following a single kick rapidly become out of phase. The oscillation of the beam is said to decohere and oscillations of the center of charge decay, leading to a reduction in the oscillation amplitude seen in the BPMs. Correction of nonlinear sources in the accelerator may remove sources of tune spread and reduce the decoherence of the beam, leading to a slower decay of the oscillation amplitude recorded by the BPMs. The lengthening of the decay of the oscillations can be used to provide a brief comparative check of the quality of a nonlinear correction. In the particular case of decoherence due to first order chromaticity, synchrotron motion leads to a periodic decoherence and recoherence of the beam motion. This occurs with a periodicity equal to that of the synchrotron motion, in the LHC this is ~200 turns.

Decoherence may also occur as a consequence of collective effects. The LHC beams utilized in the studies presented in this paper consisted of a single, low intensity, bunch. Decoherence due to collective effects was therefore not relevant to the measurements presented in this paper.

D. Dynamic aperture

The dynamic aperture (DA) defines the boundary in phase space beyond which particle motion becomes unstable. The DA is therefore of key concern for the successful operation of an accelerator and provides an excellent benchmark for the LHC nonlinear model.

One possible method to observe the dynamic aperture is to measure beam loss following large amplitude kicks. The principle behind such a measurement is illustrated in Fig. 2. A kick shifts the beam to large amplitude in z' (the angle amplitude in the plane of the kick, z denotes the position amplitude in the plane of the kick), resulting in particles passing beyond the dynamic aperture and becoming lost. The distance of the excited beam from the dynamic aperture may then be determined from the measured beam losses following the kick, while the kick amplitude itself is determined from the turn-by-turn BPM data.

The fractional beam loss is given by the integral of the charge distribution, normalized to its total charge, over the region of phase space outwith the DA. It is assumed that the charge distribution is small with respect to the dynamic aperture, such that the integral may be taken between the limits $N = \pm\infty$ (where N represents the amplitude in z, in units of $[\sigma_{\text{beam}}]$). Assuming a circularly symmetric single Gaussian charge distribution the integral is then reduced to Eq. (11), where N' represents the amplitude in z', in units of
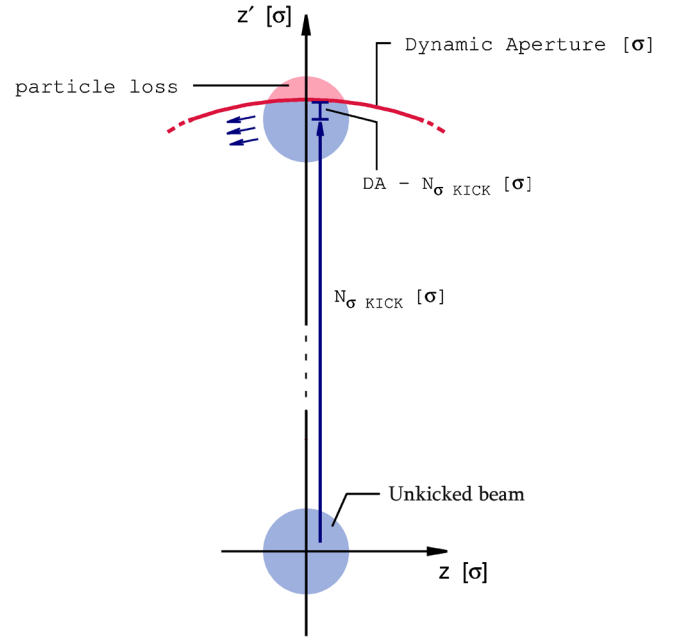

FIG. 2. Illustration of the method used to measure the dynamic aperture. The value of $(\text{DA} - N_{\sigma\text{KICK}})$ is determined from the beam loss over many turns.

$[\sigma_{\text{beam}}]$. Equation (11) can be expressed in terms of the error function, and rearranged to give an expression for the DA in terms of the measured beam loss and kick amplitude, Eq. (12).

$$\frac{\Delta I}{I} = \frac{1}{\sqrt{2\pi}} \int_{\text{DA}-N_{\sigma\text{KICK}}}^{+\infty} e^{-\frac{1}{2}N'^2} \mathrm{d}N' \qquad (11)$$

$$\frac{\text{DA} - N_{\sigma\text{KICK}}}{\sqrt{2}} = \mathbf{erf}^{-1}\left[1 - 2\frac{\Delta I}{I}\right] \qquad (12)$$

In the LHC the beams are round ($\epsilon_x = \epsilon_y$) to a close approximation and the beam size is small compared to the possible DA of the nominal machine, however there is known to be an overpopulation of the transverse tails of the charge distribution with respect to a single Gaussian distribution [26]. To limit the impact of the overpopulation of the tails on the estimate of the DA, the beam should be kicked as close to the aperture as allowed by beam losses. Alternatively the analysis of the beam losses may be extended to a more realistic charge distribution.

Losses at the dynamic and physical apertures may in general be distinguished by a consideration of the time scale over which the losses take place. Losses on a physical aperture usually occur on a time scale of a few turns, while losses upon the dynamic aperture are generally slower and occur over many turns. It is in principal possible to study the losses on a turn by turn basis using the sum signal of the BPMs, however this data was in practice unavailable. Losses during the measurements presented in this paper

were studied using the LHC Beam Current Monitors, BCT. The BCT data used have a resolution of 0.5 Hz, approximately 550 turns. While this is insufficient to allow for a completely conclusive determination of whether losses occurred on the physical aperture, it may provide a strong indication.

To definitively verify that losses are occurring at the dynamic aperture however, it is desirable to perform a second measurement with nonlinearities reduced as far as possible, while the physical aperture is unchanged. The removal of nonlinear sources may be expected to increase the DA. If a corresponding increase in the loss aperture is seen in the measurement then the dynamic aperture is the source of the observed losses. The opposite case, in which the nonlinearity is increased in order to reduce the DA, is also relevant and formed the basis of independent measurements of the DA performed on LHC Beam 1 [7,11,12].

III. MODELING THE LHC NONLINEARITY

In order to assess the understanding of the nonlinearities in the LHC measurements of the nonlinear observables described in Sec. II should be compared to simulation. To enable this, a model has been constructed in MAD-X [27] which includes the best available knowledge of the nonlinear sources in the LHC. The details of this model are described in this section.

During the LHC construction phase, measurements were performed of individual magnet misalignments within the cryostats and the alignment of the cryostats within the LHC. The Windows Interface to Simulation Errors (WISE [28]) produces estimates of the geometric errors in the LHC lattice [29] from these measurements and from known uncertainties. The geometric errors were applied in the MAD-X model.

Estimates of the magnetic errors in the LHC are also produced by WISE, based on direct magnetic measurements and on the associated uncertainties. Low current measurements were performed at room temperature on all magnets at industry (*warm measurements*), and cold measurements (under operational conditions) were performed on a fraction of the magnets once delivered to CERN. For magnets without cold measurements a *warm-to-cold* correlation is introduced in the modelling of the field, however this has an associated uncertainty. Typical uncertainties included in the WISE modeling are the uncertainty on this warm-to-cold correlation, measurement errors, hysteresis, and power-supply accuracy. A description of the production of the magnetic error estimates may be found in [30]. Magnetic errors of order (b_3, a_3) up to (b_{15}, a_{15}) were assigned to the main dipoles and quadrupoles in the LHC arcs and insertion regions. The magnetic errors produced by WISE contain both a systematic part, and a random contribution (which incorporates the uncertainties in the magnetic measurements). Sixty magnetic realisations (known as seeds) of the LHC are defined by

WISE in order to describe the likely magnetic state of the LHC. It was assumed that the b_2 errors had been well corrected during commissioning [5]. Incorporating a $\sim 10\%$ beta-beating in the model had a negligible impact on the amplitude detuning and dynamic aperture at nominal injection settings, validating the application of this assumption.

The Landau octupoles (MO) and nonlinear correctors in the LHC were set in the model to the settings present in the machine during the measurement (with the exception of the normal sextupole correctors in the arcs, the *sextupolar spool pieces*, which will be discussed shortly). Notably this includes three families of arc octupole correctors (MCO), out of a total of eight, which were malfunctioning throughout 2012 and had zero field. Adjustments were then applied to the settings of the MCO in order to reproduce a best estimate of their substantial hysteresis effects, which studies in 2011 determined were an important contribution to the Q'' of the bare machine [8,31].

The normal sextupolar correctors (MCS) are intended for the compensation of b_3 errors in the LHC arcs. The settings of elements present in the machine were not applied directly to the model. There is a dynamic component to the sextupolar errors in the LHC which is not included in the WISE seeds, and corrections for the dynamic b_3 are included in the machine settings of the MCS. The compensation of the dynamic b_3 was therefore assumed to be perfect, and corrections for the static b_3 defined in the WISE seeds applied to the MCS in the model. It is worth highlighting that the quality of the local b_3 correction in the LHC arcs has never been checked with beam, and represents a potential limitation on the understanding of the nonlinear dynamics via higher order sextupole perturbations.

In addition to the geometric errors defined by WISE, in 2011 there were possible indications of a slight (< 0.1 mm) systematic horizontal misalignment of the arc decapolar correctors with respect to the arc dipoles [8,32]. These observations were not conclusive, but could explain a significant proportion of the missing Q'' in the bare machine [8,32]. The contribution to the detuning (of the order 1×10^3 m^{-1}) was small at nominal injection settings.

Tunes and chromaticities were matched to the measured values. The closed orbit was matched toward a zero reference orbit, but retained a realistic *root mean square* in the arcs. Crossing and separation bumps through the LHC insertions which were present during the experiment were reproduced in the model.

It has been observed in simulations of detuning with amplitude at top energy in the LHC, that the linear coupling could significantly influence the nonlinear phenomenology of the machine [23]. The quality of the linear coupling model is therefore a particular concern for study of the nonlinear dynamics. Linear coupling is characterized by the magnitude of the f_{1001} resonance driving term (RDT),

which drives the $(Q_x - Q_y)$ resonance, and varies around the LHC ring. The global quantity $|C^-|$ is related to the mean amplitude of the RDT around the accelerator ring $(\overline{|f_{1001}|})$ by Eq. (13), [33].

$$|C^-| = 4|(Q_x - Q_y)|\overline{|f_{1001}|} \qquad (13)$$

The value of f_{1001} in the LHC BPMs was determined from spectral analysis of turn-by-turn data obtained following small amplitude ($\sim 2\sigma$) kicks. A small kick was used for the determination of f_{1001} in order to avoid any amplitude dependent contribution. The mean amplitude of the f_{1001} was extremely stable throughout the measurements described in this paper, however there were significant local variations of $|f_{1001}|$ around the ring. The local fluctuations in the amplitude of the RDT corresponded to an equivalent range of $0.002 \leq |C^-| \leq 0.004$ (it should be emphasized that the range in $|C^-|$ quoted is an equivalent to the f_{1001} fluctuation, intended to give a sense of the scale of the local variation of the RDT, rather than an actual change of $|C^-|$ which is a global quantity).

The best procedure would be to reproduce the linear coupling in the model by locally matching to the measured f_{1001} around the ring. This is not currently implemented for the LHC model and applying the measured a_2 errors does not guarantee the correct local f_{1001}. In the MAD-X model therefore, a_2 errors were not included, this gave a relatively flat $|f_{1001}|$ around the ring. The linear coupling was then matched using the LHC global coupling knobs [34] in order to produce a given phase and amplitude of f_{1001} in the center of Arc12 (the LHC arc located between Insertion Regions 1 and 2, which house the ATLAS and LHCb experiments, respectively). In order to assess the uncertainty in the nonlinear observables due to the linear coupling ~ 2000 random realizations of the LHC were then defined. The $|f_{1001}|$ was defined on an even distribution within the band defined by the observed local fluctuations of the RDT. The phase of f_{1001} at the matching location was varied randomly with a uniform distribution. The sixty seeds defined by the WISE magnetic model were also varied randomly with a uniform distribution. Evidently this is a somewhat artificial construct, in reality the $|f_{1001}|$ and its phase vary around the ring according to the distribution of a_2 sources, however the purpose is to assess the uncertainty arising in the nonlinear observables due to the variation of f_{1001} around the ring, not to directly reproduce this effect in the model.

The nonlinear observables measured with kicked beams, as described in Sec. II, can be simulated in this model by tracking particles initially displaced from the closed orbit. Both the Polymorphic Tracking Code (PTC [35]) module within MAD-X, and SIXTRACK [36], were used for such simulations. The PTC Normal module in MAD-X also provides a convenient way to determine the detuning with amplitude and the nonlinear chromaticity.

For the model of the nominal injection optics no matching of the nonlinear parameters is performed. The model therefore represents the current understanding of the nonlinear sources. All comparisons between measured and simulated nonlinear observables presented in this paper utilize this model.

Nonlinear parameters of the model, in particular the nonlinear chromaticity and detuning with amplitude, may be matched to produce a so-called "effective model," which reproduces observed properties of the machine. As will be described in Sec. IV B 2, this has been done for the state of the machine in the latter half of the experiment, where departures from the nominal magnetic cycles of the octupolar correctors in the arcs made estimates of the hysteresis errors in these elements impractical. Such matchings were performed in MAD-X using macros which call the PTC normal module.

IV. MEASUREMENTS OF NONLINEAR OBSERVABLES PERFORMED ON THE LHC BEAM 2 AT INJECTION

A. Experimental procedure

Measurements of the nonlinear observables described above require large amplitude excitation of the beam. The LHC aperture kicker used to provide the excitation for these studies represents a considerable safety risk to the LHC machine. Consequently, machine accesses were required at the start and end of measurement period to physically enable and disable the MKA in the LHC tunnel. Single probe bunches were used for the measurement which had intensities ($\sim 1 \times 10^{10}$ protons) below the damage threshold of the LHC. The collimators in the LHC were retracted from their operational settings in order to allow measurements out to large amplitudes. The horizontal and vertical primary collimators were left at $11.6\sigma_{nominal}$ (where $\sigma_{nominal}$ is defined as corresponding to a normalized emittance of $3.75~\mu m$) in order to shield the LHC triplets, all other collimators were retracted beyond this aperture.

An initial series of measurements were performed on LHC Beam 2 at nominal injection optics, with kicks applied in either the horizontal or vertical planes. Multiple kicks were performed, with amplitude increasing incrementally up to the limit defined by beam losses. A distinct experiment was performed on LHC Beam 1 in parallel with the studies described in this paper [12], as such all results presented in the following sections pertain to measurement of LHC Beam 2.

Following a successful series of measurements at nominal injection settings, the Landau octupoles (MO) were powered to zero, and the MCO were driven to their zero field settings. Corrections for the second and third order chromaticities found during the 2011 nonlinear measurement program were then applied. A second series of kicks were then performed on this *corrected* machine in the

horizontal, vertical, and diagonal planes. As in the case of the nominal measurement series, the kick amplitudes were increased incrementally out to the maximum defined by beam losses.

Unperturbed tunes, first order chromaticities, and linear coupling were very stable throughout the measurement. The value of Q' was ~2 (the nominal value for the LHC) in both planes throughout the experimental period. The tunes also remained close to their nominal values (0.28 and 0.31 in the horizontal and vertical planes, respectively). The only substantial change was observed in Q_y following a beam-protection dump during measurements of the corrected machine. After recovery, the vertical tune was corrected to a value 0.0027 smaller than had previously been present in the machine. A correction has been applied to the detuning data to compensate for this shift. Emittance measurements of the unkicked beams were performed regularly throughout the experiment, this too was found to be extremely stable.

B. Experimental results and their comparison with simulation

1. Decoherence

As described in Sec. IV A, following amplitude detuning and DA measurements at nominal injection settings Landau octupoles were powered to zero and Q'' and Q''' corrections, found in 2011, were applied. A check of the effectiveness of the 2011 nonlinear chromaticity corrections was required before proceeding with the remainder of the study, however, due to a parallel experiment running on Beam 1, direct verification of the correction via measurement of Q with $\frac{\Delta p}{p_0}$ was not possible. To perform a brief check of the correction quality therefore, small $(2\sigma_x, 2\sigma_y)$ kicks were performed at nominal injection settings, following the depowering of the MO to zero and zeroing of the MCO field, and after inclusion of the 2011 nonlinear chromaticity corrections. The decoherence of the three kicks were compared. This is shown in Fig. 3.

The decoherence of the kicked beam was substantially reduced by the depowering of the MO to zero together with the zeroing of MCO residual fields, and again on the application of the 2011 nonlinear chromaticity corrections. This qualitatively indicated the 2011 corrections were still valid, and the experiment proceeded using this new configuration. It is also interesting to observe that upon correction of the octupolar and decapolar nonlinearities (blue data) a periodic beating of the decoherence pattern is revealed, corresponding to the decoherence due to first order chromaticity together with the synchrotron motion.

2. Amplitude detuning

As described in Sec. IV A amplitude detuning measurements were performed at nominal injection settings, and at the corrected optics. During the nominal measurement only
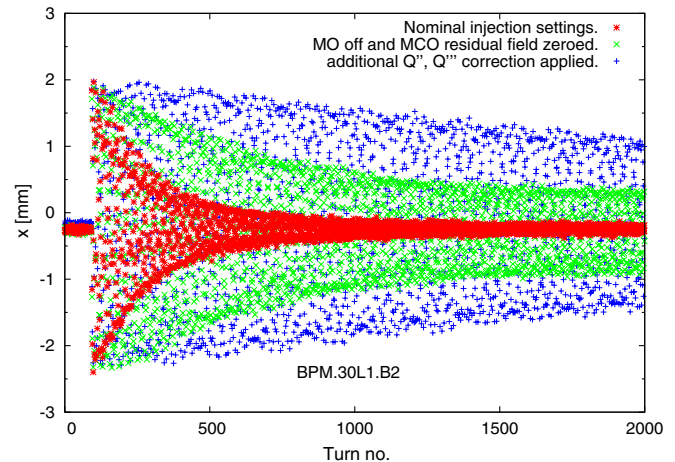

FIG. 3. Decoherence of $(2\sigma_x, 2\sigma_y)$ kicks at injection. The decoherence of kicks at the three different optics studied are shown: nominal injection settings settings (red), with Landau octupoles powered to zero and the MCO residual field zeroed (green), and the corrected configuration with Q'' and Q''' corrections applied on top of the preceding state (blue).

horizontal or vertical kicks were applied (together with small excitations in the opposite plane to ensure successful tune measurements), however coupling of the kicks into the opposite plane did occur. Attempting to fit the 2D Taylor expansion up to second order, Eq. (1), fails in this case due to a lack of data in the diagonal plane. As described in Sec. II A the quality of the fit can be checked qualitatively by comparing detuning terms in the expansion of Q_x and Q_y which are by definition identical. These values differed significantly in the 2D fit, implying the detunings calculated by this method were unphysical. This is not unexpected. The second order diagonal term does not influence pure horizontal or vertical detuning, and was only weakly constrained by the data due to the coupling of large kicks into the opposite plane. Under such conditions its inclusion in the regression model is inappropriate and can be expected to reduce the fit quality. A regression without the diagonal term, equivalent to the 1D analysis of Eq. (5), is more suitable to the available data.

Making the approximation to 1D Taylor expansions, Eq. (5), requires that some data is excluded from the fit due to a substantial coupling of the highest amplitude vertical kick into the horizontal plane (this coupling is discussed in more detail in the following section). The calculated detunings are given in Table III(a). First order cross terms of the Q_x and Q_y fits, Eq. (6), agree well.

When measuring the detuning with amplitude of the corrected configuration the beam was kicked horizontally, vertically, and diagonally. In this case fitting to the 2D Taylor expansion, Eq. (1), is feasible. Table III(b) presents the results of the fits to measured data for this configuration. The measured detunings are consistent with Eq. (6) and Eq. (7).

TABLE III. Results of fits to measured amplitude detuning.

(a) Nominal injection settings. 1D polynomial fits.				(b) MO off, and Q'', Q''' corrections applied. Fits to 2D Taylor expansions.			
Anharmonicity	[unit]	Fit	± Fit error	Anharmonicity	[unit]	Fit	± Fit error
Q_x (from J_x fit)	[tune units]	0.2821	20×10^{-5}	Q_x	[tune units]	0.28061	6×10^{-5}
Q_y (from J_x fit)		0.3124	10×10^{-5}	Q_y		0.31151	2×10^{-5}
Q_x (from J_y fit)		0.28035	9×10^{-5}	$\cdots$			
Q_y (from J_y fit)		0.31409	1×10^{-5}	$\cdots$			
$\frac{\partial Q_x}{\partial \epsilon_x}$	$[10^3 \text{ m}^{-1}]$	-29	7	$\frac{\partial Q_x}{\partial \epsilon_x}$	$[10^3 \text{ m}^{-1}]$	0.8	1
$\frac{\partial Q_y}{\partial \epsilon_x}$		19	3	$\frac{\partial Q_y}{\partial \epsilon_x}$		-1.4	0.4
$\frac{\partial Q_x}{\partial \epsilon_y}$		24	4	$\frac{\partial Q_x}{\partial \epsilon_y}$		-2.0	0.7
$\frac{\partial Q_y}{\partial \epsilon_y}$		-32.8	0.4	$\frac{\partial Q_y}{\partial \epsilon_y}$		2.8	1
$\frac{\partial^2 Q_x}{\partial \epsilon_x^2}$	$[10^9 \text{ m}^{-2}]$	-60	30	$\frac{\partial^2 Q_x}{\partial \epsilon_x^2}$	$[10^9 \text{ m}^{-2}]$	-18	5
$\frac{\partial^2 Q_y}{\partial \epsilon_x^2}$		34	10	$\frac{\partial^2 Q_y}{\partial \epsilon_x^2}$		6	1
$\frac{\partial^2 Q_x}{\partial \epsilon_y^2}$		11	34	$\frac{\partial^2 Q_x}{\partial \epsilon_y^2}$		11	3
$\frac{\partial^2 Q_y}{\partial \epsilon_y^2}$		-13	3	$\frac{\partial^2 Q_y}{\partial \epsilon_y^2}$		-20	3
$\cdots$				$\frac{\partial^2 Q_x}{\partial \epsilon_x \partial \epsilon_y}$		7.6	3
$\cdots$				$\frac{\partial^2 Q_y}{\partial \epsilon_x \partial \epsilon_y}$		8	3

Figure 4 plots $Q_{x,y}(\epsilon_x, \text{const})$ and $Q_{x,y}(\text{const}, \epsilon_y)$ as determined from the fits described above. Results from the nominal injection setting measurement are shown in red, and results from the corrected configuration measurement are shown in blue. Uncertainties on the fit are indicated in grey. The measured tunes for the horizontal and vertical kicks are also shown, plotted against the measured $\epsilon = 2J$ of the kick in the dominant plane. The highest amplitude vertical kick during the nominal measurement is plotted in black, this is to indicate it was excluded from the fit due to a significant coupling into the opposite plane.

The amplitude detuning in the nominal case is substantial. Considering the tune shift with ϵ_x (Fig. 4, left), by a kick amplitude of $\sim 8.3\sigma_{x\,\text{nominal}}$ Q_x and Q_y are driven toward the fourth and third order resonances, respectively. This is well illustrated by Fig. 5 which plots the turn-by-turn position and phase-space at an LHC arc BPM following the $(8.3\sigma_x, 0.6\sigma_y)$ kick. The three and four island structures corresponding to these resonances are evident. Regarding the approach of the tune to these resonances, it is insufficient to consider only the first order amplitude detuning. Higher order detuning terms are large, and are observed to impact significantly the detuning over the amplitude range studied, including within the $5.7\sigma_{\text{nominal}}$ aperture defined in operation by the collimators.

With respect to the tune shift with ϵ_y in the nominal case, the first order detuning is again substantial, but drives the tunes together. Second order detunings with ϵ_y are not so substantial as with ϵ_x, however, as will be discussed in the

following section, amplitude dependent coupling plays an important role at large amplitudes in the vertical plane.

Following the depowering of the Landau octupoles to zero, and the application of corrections for the nonlinear chromaticities, the detuning with amplitude is significantly smaller. Magnitudes of the first order terms were reduced by factors between 10 and 30, and second order detunings with ϵ_x were reduced by factors 3 and 5. $\partial^2 Q_x/\partial \epsilon_y^2$ was unaffected by the depowering of the Landau octupoles and subsequent nonlinear chromaticity correction, but had been small initially. $\partial^2 Q_y/\partial \epsilon_y^2$ increased by $\sim 50\%$, but had a post-correction magnitude comparable with that of the $\partial^2 Q_x/\partial \epsilon_x^2$ (which had been reduced considerably). Losses upon kicking the beam were reduced and it was possible to perform kicks out to higher amplitudes than at nominal optics. No important resonances were approached within the available aperture.

As described in Sec. III, the uncertainty in the simulated nonlinear observables is significantly influenced by the quality of the linear coupling model. It is not, at present, possible to reproduce the local coupling (as characterized by the f_{1001} resonance driving term) in the model. The uncertainty in the simulated nonlinear observables is therefore assessed by producing LHC models with flat $|f_{1001}|$ around the ring, and analyzing ~ 2000 realizations of this model, distributed in $|f_{1001}|$ to reproduce the observed coupling (the coupling phase and the WISE seed were varied randomly on a uniform distribution). This procedure was described in Sec. III.
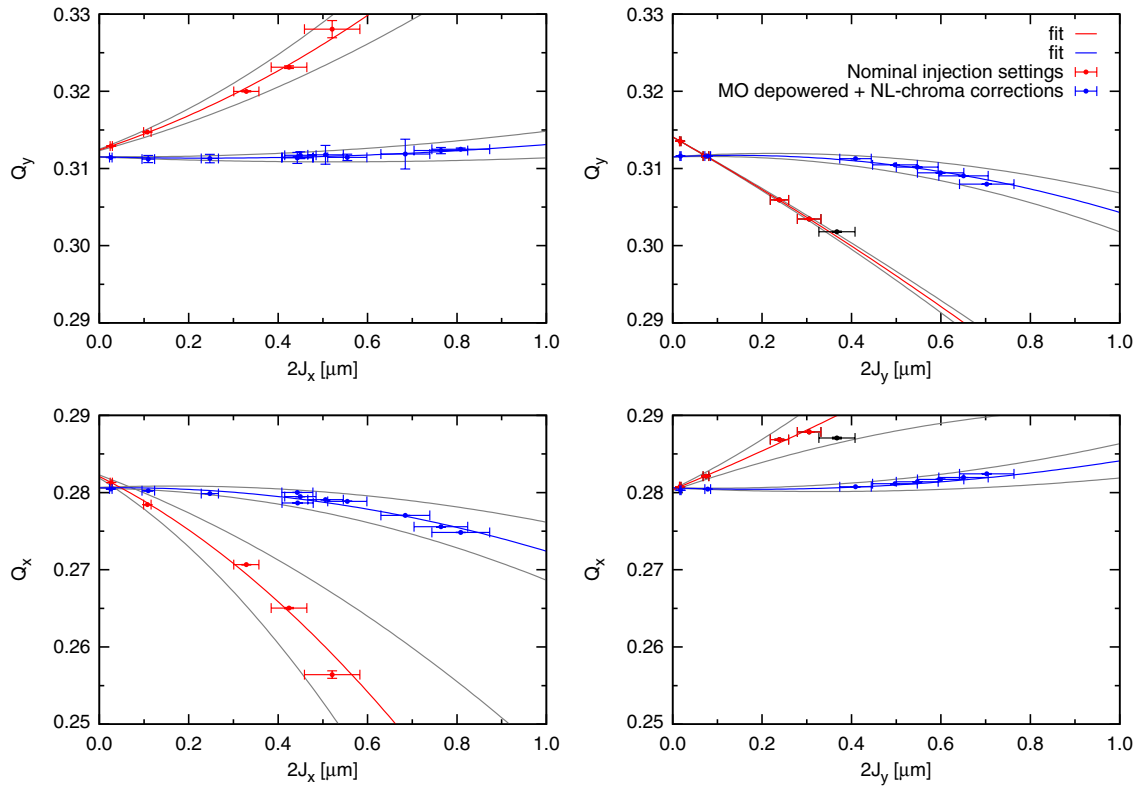
FIG. 4.   Detuning with amplitude of the LHC at nominal injection settings (red), and with Landau octupoles set to zero and additional corrections for Q'' and Q''' applied (blue). The tune is plotted against the horizontal and vertical single particle emittance of the kicks. Points shown in black represent kicks where there was substantial coupling of the kick into the opposite plane.
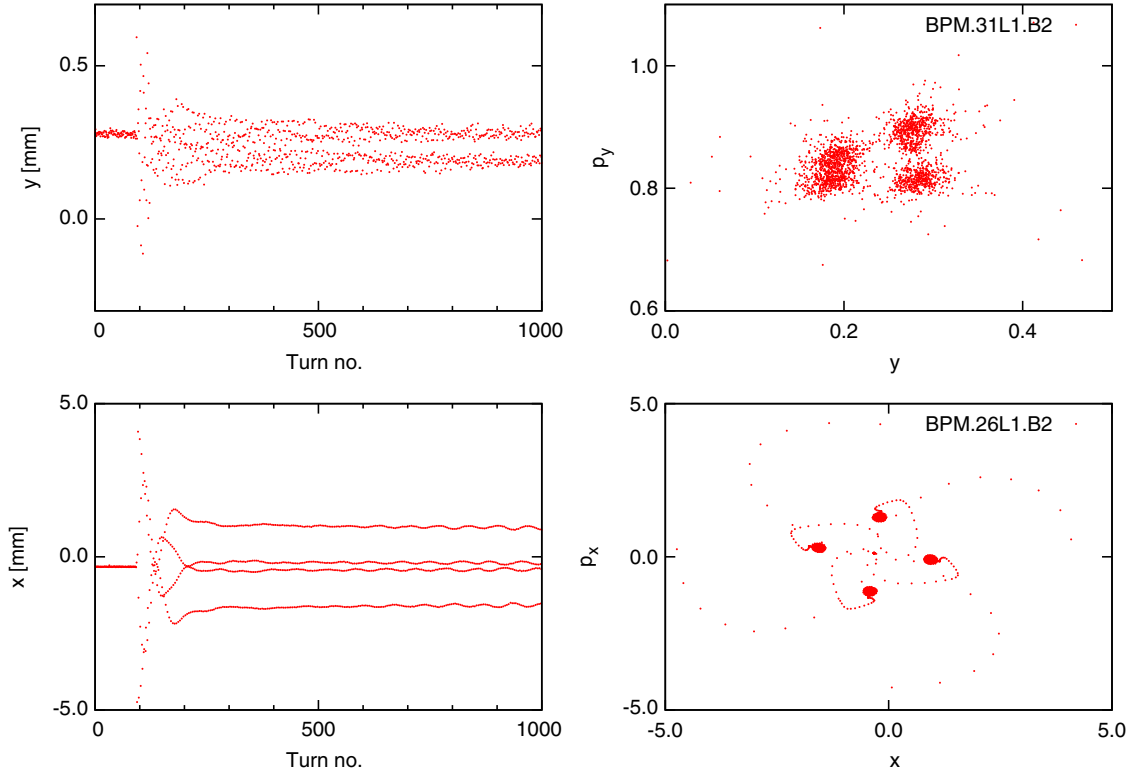

FIG. 5.   Turn-by-turn (TbT) and phase space data for a $(8.3\sigma_x, 0.6\sigma_y)$ kick with nominal LHC injection settings in the vertical plane at BPM.31L1.B2 (top), and the horizontal plane at BPM.26L1.B2 (bottom).
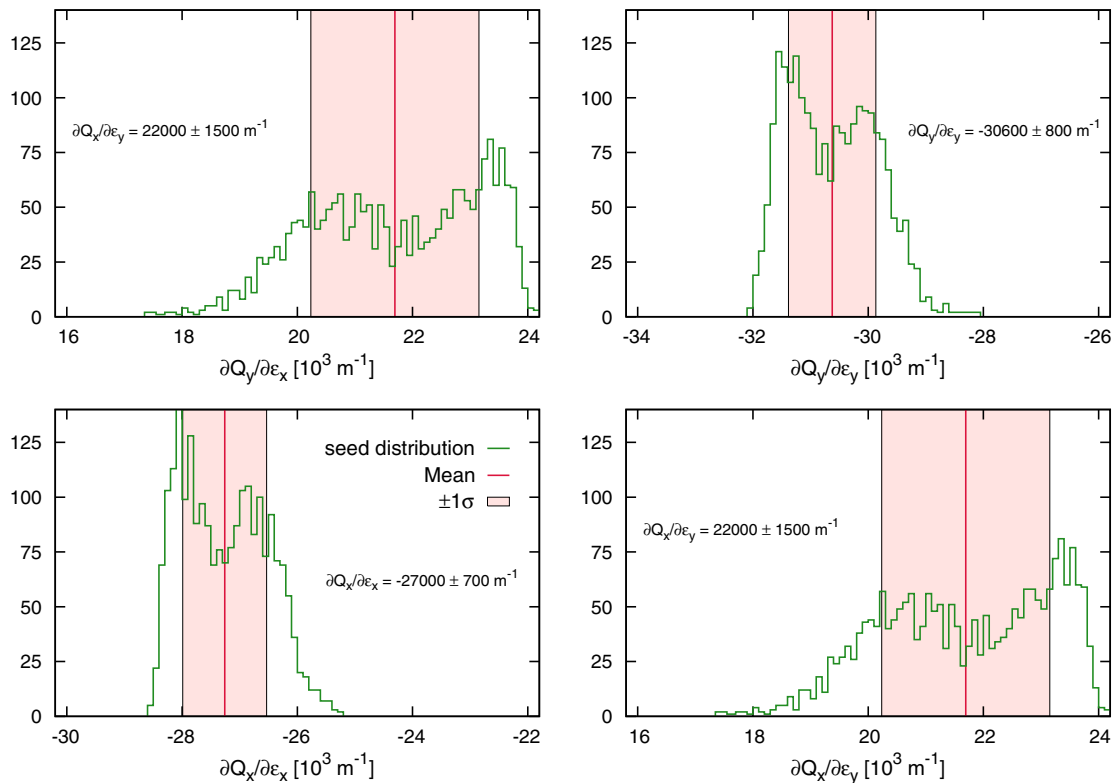
FIG. 6. Histogram showing the distribution of first order detuning with amplitude of ~2000 random instances of the LHC, with $|f_{1001}|$ defined on an even distribution within the band defined by measurements of local fluctuations of the RDT around the LHC ring, and a uniform distribution in the phase of f_{1001} at the matching location. The WISE seeds were also varied randomly on a uniform distribution.

Figure 6 displays histograms of the first order detunings of the 2000 realizations of the LHC considered. The mean and standard deviations of the distribution are indicated. Both the $|f_{1001}|$ and the phase at the matching point playing an important role in the uncertainty in the detuning with amplitude. There was also a small contribution from the uncertainties in the magnetic model. In light of the significant impact the f_{1001} resonance driving term appears to have on the detuning, it may be important in future nonlinear studies to investigate the feasibility of matching locally to a measured f_{1001}.

Table IV compares the modeled and measured amplitude detunings. As the first order detuning at nominal injection settings is dominated by the Landau octupoles the good agreement between the modeled and measured first order amplitude detuning may be expected: nonetheless this is an important verification of the nonlinear LHC model.

In contrast to the first order case there are more substantial differences in the second order detunings. While the modeled values show a qualitatively similar behavior to the observations ($\partial^2 Q_x / \partial \epsilon_y^2$ has the opposite sign, but both modeled and measured magnitudes are small enough that their contributions are slight within the amplitude range of interest, and both model and measurement have substantial relative uncertainties), there are quite considerable deficits with respect to the measurements.

Over the amplitude range examined the discrepancies between the model and the measurement have a relevant effect, and in particular result in Q_y reaching the third order resonance at a horizontal amplitude $0.7 \pm 0.6 \sigma_{\text{nominal}}$ larger than was measured (as calculated from the mean and standard deviation values of the first and second order detuning). Likewise there is a similar effect in the approach of Q_x to the fourth order resonance. This may indicate that

TABLE IV. Comparison of modeled and measured detuning with amplitude at nominal injection settings.

Detuning	[unit]	Measured	$\pm$ error	Model	$\pm$ error
$\frac{\partial Q_x}{\partial \epsilon_x}$	$[10^3 \ \text{m}^{-1}]$	-29	7	-27.0	0.7
$\frac{\partial Q_y}{\partial \epsilon_x}$		19	3	22	1.5
$\frac{\partial Q_x}{\partial \epsilon_y}$		24	4	22	1.5
$\frac{\partial Q_y}{\partial \epsilon_y}$		-32.8	0.4	-30.6	0.8
$\frac{\partial^2 Q_x}{\partial \epsilon_x^2}$	$[10^9 \ \text{m}^{-2}]$	-60	30	-14	3
$\frac{\partial^2 Q_y}{\partial \epsilon_x^2}$		34	10	17	8
$\frac{\partial^2 Q_x}{\partial \epsilon_y^2}$		11	34	-10	9
$\frac{\partial^2 Q_y}{\partial \epsilon_y^2}$		-13	3	-3	4

second order perturbations of the octupoles in the LHC are being underestimated in present models.

An attempt was not made to model the corrected configuration of the LHC only from knowledge of the machine state. Deviations from the standard hysteresis cycle of the MCO meant their field was uncertain, and there are still some unidentified sources of detuning and Q'', seen in 2011, which may become significant when the Landau octupoles are less strongly powered. The corrected optics was instead simulated in MAD-X by reproducing, on top of the nominal model, the trims applied to the MO, MCO, and MCD and then matching settings of the octupolar elements in order to reproduce the measured amplitude detuning. This model was used to simulate the dynamic aperture of the corrected machine configuration, as described in Sec. IV B 4.

As discussed in Sec. II A, the use of Eq. (4) to determine the action of applied kicks is an approximation if the phase space trajectory is distorted away from an ellipse. At the corrected configuration the small detuning with amplitude resulted in the tunes not approaching any important resonances within the amplitude range examined, and the phase space was not significantly distorted away from an ellipse. This was further verified by observing an excellent agreement of the detuning with amplitude in the matched model of the corrected configuration as determined from ptc_normal (which correctly handles nonlinear distortion of phase space) and from tracking simulations using Eq. (4). The use of Eq. (4) was therefore deemed justified for the study of the corrected configuration.

Having determined that Eq. (4) was valid for the corrected configuration, the validity to the nominal LHC optics was assessed by comparing the action of the applied MKA kicks, determined using Eq. (4), measured at both the nominal and corrected configurations. The MKA is known to have good magnetic reproducibility, discrepancies between the action measured at the two configurations would therefore indicate that Eq. (4) is no longer reliable. In the horizontal plane a discrepancy was observed for the two highest amplitude kicks at the nominal optics, corresponding to the approach of the horizontal and vertical tunes to the fourth and third order resonances, however the discrepancy was well within the uncertainty on the measured action. In the vertical plane no significant discrepancy was observed, with the exception of the highest amplitude kick at nominal optics. This discrepancy was within the measurement uncertainty, and as has been previously discussed this kick had already been excluded from the determination of the detuning with amplitude due to the significant coupling of the vertical kick into the horizontal plane. The use of Eq. (4) for the studies of the nominal LHC optics described in this paper was therefore deemed justified.

The results presented here represent a partial, but important, verification of the nonlinear model in respect to the amplitude detuning. The consistency between model and measurement is good for the first order terms, while the higher order contributions show a qualitatively similar behavior. Amplitude ranges relevant to operation are smaller than those considered in the nonlinear study presented here (collimators in operation define an aperture of $\sim 5.7\sigma_{\text{nominal}}$). At lower amplitudes the second order detuning plays a smaller role, though it is still significant.

Bearing in mind the discrepancies of higher order terms it is now possible to use the nonlinear model to consider operational settings of the LHC and potential scenarios which have not been studied directly. The implications of these detuning observations for a revised injection optics with reversed Landau octupole polarity which was introduced in the latter half of 2012, and for a suggested injection Landau octupole configuration for 25 ns bunch spacing, were discussed briefly in [32]. To better understand the observations, particularly of second order detunings, further studies will be required along with an improved method of modeling the linear coupling in the machine.

3. Nonlinear coupling

The linear coupling measured by the LHC BBQ [25,37] during these studies was stable at $|C^{\pm}| \approx 0.002$ throughout the experiment ($C^{\pm}$ indicates the BBQ measures a mixture of C^{+} and C^{-}, which in the LHC is dominated by the C^{-}). This value is consistent, via Eq. (13), with the $|f_{1001}|$ at BPMs close to the BBQ position on the LHC ring. In parallel with the nonlinear dynamics experiment, the regular injections of LHC Beam 2 required during these studies were used to demonstrate the measurement of linear coupling (as determined from f_{1001}) using injection oscillations [10]. The linear coupling RDT measurements, which were obtained by this method for every injection during the experiment, were consistent with the BBQ and kicked beam values, and showed the f_{1001} to be very steady. Linear coupling was therefore small (in the range 0.002 to 0.004) and stable throughout these measurements.

Difference linear coupling (C^{-}, driven by the f_{1001} resonance driving term) defines a closest approach of the normal mode tunes, Eq. (14).

$$|\delta Q_{\min}| = |C^{-}| \qquad (14)$$

On applying vertical kicks to the beam at nominal injection optics, the detuning with amplitude forced the horizontal and vertical tunes together. Figure 7 plots the measured (green) and the modeled (blue) tune split, $|Q_x - Q_y|$, against the action of applied vertical kicks. The modeled tune split was examined by tracking kicked particles in the nonlinear model described in Sec. III. The linear coupling in the model was matched to $\delta Q_{\min} = 0.006$, to avoid any underestimation of the role played by linear coupling. In both modeled and measured
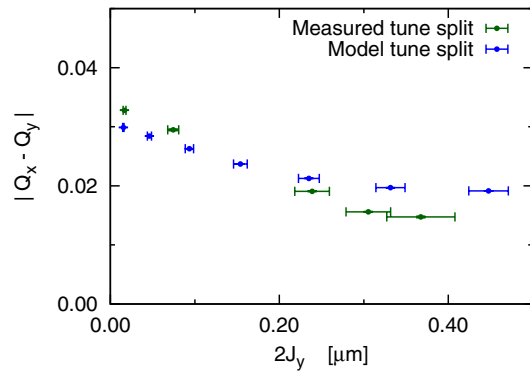
FIG. 7.   Modeled and measured variation in the tune-split with vertical kick amplitude at nominal injection optics.

cases the separation of the tunes appear to approach a minimum, however the observed value, $\delta Q_{\min} \sim 0.015$ (Model: ~ 0.02), is significantly larger than possible due to linear coupling.

Coupling between the transverse planes results in periodic emittance transfer, and hence the familiar beating of the betatron oscillations. Assuming any external excitation is kept constant in one plane, coupling may be identified by a growth of $\epsilon_{\max}$ in the unkicked (or minimally kicked) plane with increasing excitation in the dominant plane. When the transverse planes are fully coupled, $\Delta = 0 \rightarrow |Q_x - Q_y| = \delta Q_{\min} = |C|$ (where Δ is the unperturbed tune split and $|Q_x - Q_y|$ is the separation of the normal mode tunes which are measured in the machine), the emittances are completely shared and $\epsilon_{\max\,x} = \epsilon_{\max\,y}$. This does not violate conservation of phase space volume as the peak ϵ of one plane corresponds with the minimum ϵ of the other.

Equation (4) calculates $\epsilon_{\max}$, which in the absence of coupling defines the action of the kick. Figures 8 and 9 plot
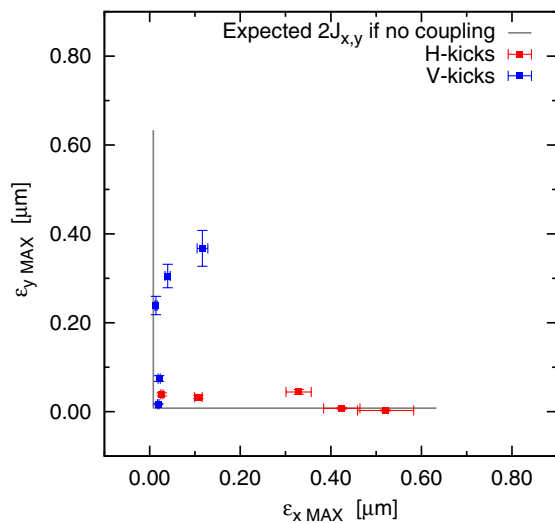
FIG. 8. $\epsilon_{\max}$ calculated using Eq. (4) for the horizontal and vertical kicks applied during amplitude detuning measurements at nominal injection optics.
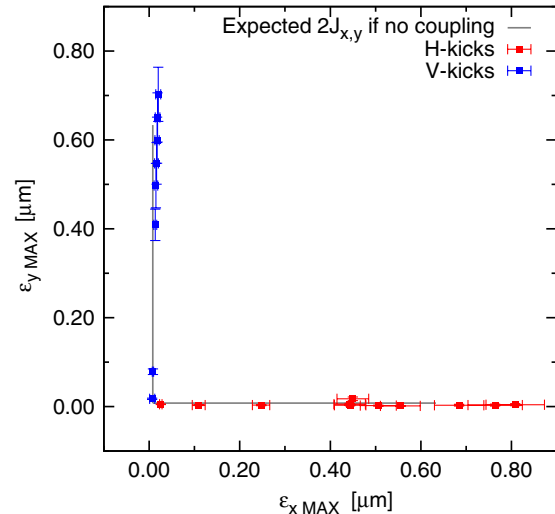
FIG. 9. $\epsilon_{\max}$ calculated using Eq. (4) for the horizontal and vertical kicks applied during amplitude detuning measurements with Landau octupoles depowered to zero and Q'' and Q''' corrections applied.

$\epsilon_{\max}$, calculated using Eq. (4), in the (ϵ_x, ϵ_y) plane for the horizontal and vertical kicks applied during the amplitude detuning measurements. Figure 8 plots the results for measurements at nominal injection optics, Fig. 9 plots the results for measurements at the corrected optics with MO depowered to zero, and Q'' and Q''' corrections applied.

Considering the vertical kicks applied at nominal injection optics, Fig. 8, as vertical kick amplitude is increased there is substantial growth of $\epsilon_{x,\max}$. At the largest amplitudes examined $\epsilon_{x,\max}$ becomes comparable with the action of the vertical kick. This is a strong indication that the transverse planes are significantly coupled, which should not be the case when the tune split is so much greater than the linear $|C^-|$. Equivalent behavior is not observed at the corrected optics. This rules out any systematic effect of the MKA as the source of this growth.

A similar behavior to that observed in Fig. 8 is also seen in simulation. This is shown in Fig. 10 which compares the measured $\epsilon_{\max}$ (green) with the modeled $\epsilon_{\max}$ of tracked particles (red, blue). Examining the simulated tracking data it was seen that the growth of $\epsilon_{\max}$ in the unkicked plane was the result of beating of the betatron oscillations between the transverse planes, and was therefore driven by transverse coupling.

Due to the rapid decoherence of large amplitude kicks at nominal injection optics, any clear beating of the measured betatron oscillations is obscured for the kicks of interest. Considering Fig. 11 however, which displays an example of the turn-by-turn data obtained at a BPM following a large amplitude vertical kick, some important qualitative features are observable. The amplitude of the small horizontal kick is well understood, measurements at the corrected optics showing an excellent agreement with theoretical predictions at small amplitudes [10].
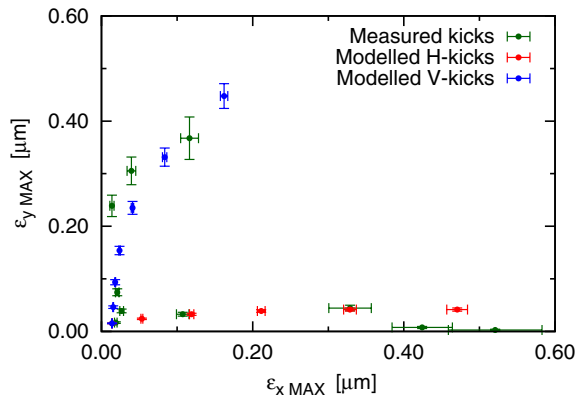
FIG. 10. Comparison of the modeled and measured ϵ_{MAX} of kicks in the horizontal or vertical planes at nominal injection optics.

The amplitude of the horizontal and vertical kicks are indicated in Fig. 11. Following the application of the kicks the betatron oscillation amplitude in the horizontal plane shows a rounded growth then decay up to a value considerably in excess of the initial horizontal excitation. Such an observation is characteristic of emittance exchange due to coupling. The decay of the oscillations due to decoherence of the kick is also unusual: the sudden change of gradient in the horizontal decay, near turn 150, appears to suggest the superposition of a large but rapidly decaying mode of oscillation, with a smaller longer lived mode. This would be consistent with coupled motion given the disparity in amplitude between the kicks, and the strong nonlinearities present in the machine at nominal injection optics (which result in far more rapid decoherence of large kicks).

The earlier described growth of $\epsilon_{x,\text{max}}$ with vertical kick amplitude is a convincing signal of coupled motion. The
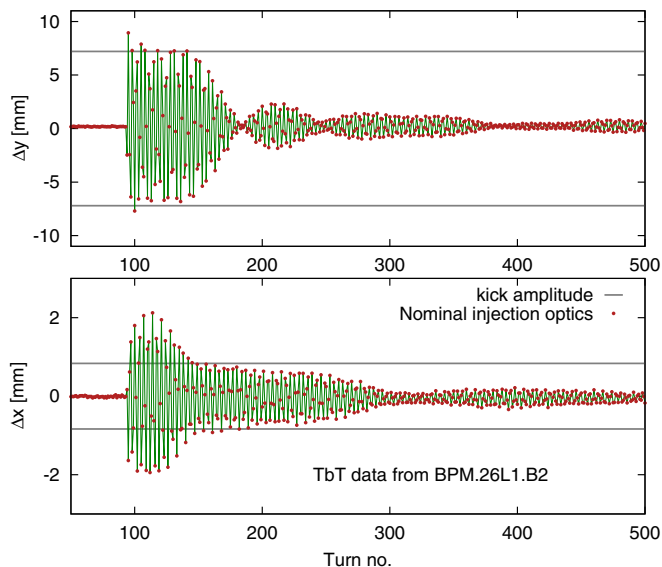
FIG. 11. Measured TbT data from a large amplitude vertical kick at nominal injection optics.

qualitative features of Fig. 11 just described are additional indications. That the δQ_{min} in the model corresponds with the transverse planes becoming coupled is clear from the growth of $\epsilon_{x,\text{max}}$ with vertical kick amplitude and an associated beating of the betatron oscillations of tracked particles. This can also be demonstrated in simulation by showing that a δQ_{min} is not approached if the initial tune split is increased. This is shown in Fig. 12.

As has been described in this section, the linear coupling was independently measured by the LHC BBQ and by spectral analysis of low amplitude betatron oscillation data. The two measurements were consistent, and the linear $|C^-|$ was determined to be in the range 0.002 to 0.004. On kicking the beam to large vertical amplitudes, a $\delta Q_{\text{min}} = 0.015$ was approached. This δQ_{min} is significantly in excess of the linear $|C^-|$. An observed increase of the peak emittance in the horizontal plane with vertical kick amplitude, together with the qualitative features of the raw turn-by-turn data, indicate this was a δQ_{min} driven by coupling. It is concluded therefore, that an amplitude dependent (nonlinear) coupling between the transverse planes of the LHC, giving rise to an amplitude dependence of the δQ_{min}, has been observed.

Similar nonlinear coupling effects are reproduced in the LHC model, namely the approach to a δQ_{min} (comparable with measurement) which is significantly in excess of the precisely known linear $|C^-|$. Growth of the peak emittance in the unkicked plane was consistent with measurements, and the beating of the betatron oscillations of tracked particles clearly identified coupling as the source of this growth. It was shown that on increasing the initial tune separation no saturation of the tune split was observed over the same amplitude range.

In light of these observations a new avenue has been opened through which the LHC dynamics may be studied. The respectable agreement between the simulated and measured nonlinear coupling now allows for the use of
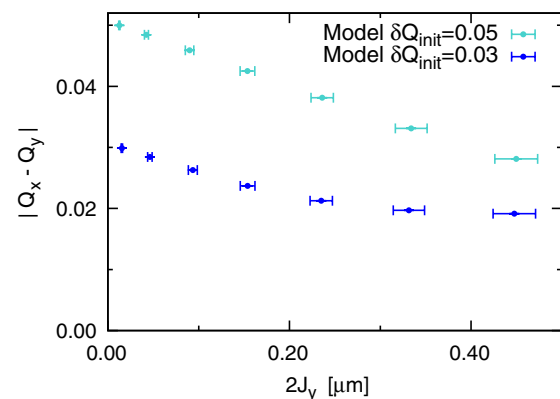

FIG. 12. Variation of the simulated tune split ($|Q_y - Q_x|$) with the action of vertical kicks at nominal injection optics. This is shown for the nominal tune split with unkicked beams, and for an increased initial separation of the tunes.

the nonlinear LHC model in the determination of the dominant sources, and further studies are underway with the aim of studying the reported effect in more detail. In the meantime however, the studies presented here represent a further validation of the understanding of the LHC nonlinearities.

4. Dynamic aperture

As described in Sec. II D it is possible to determine the distance of the beam from an aperture by examining the beam losses. If the beam is excited with a kick it is possible to obtain the amplitude of excitation using Eq. (3) and Eq. (4). Together such measurements allow a determination of the aperture. As a result, the large amplitude excitations applied to measure the amplitude detuning also present the opportunity to study the LHC dynamic aperture. Figure 13 plots the surviving beam intensity 30 s after the application of a kick with the LHC MKA, as a function of the kick amplitude in units of $\sigma_{\mathrm{nominal}}$.

It is clear from the increasing losses with increasing kick amplitude that in all cases considered the beam is being driven toward an aperture. Following correction of
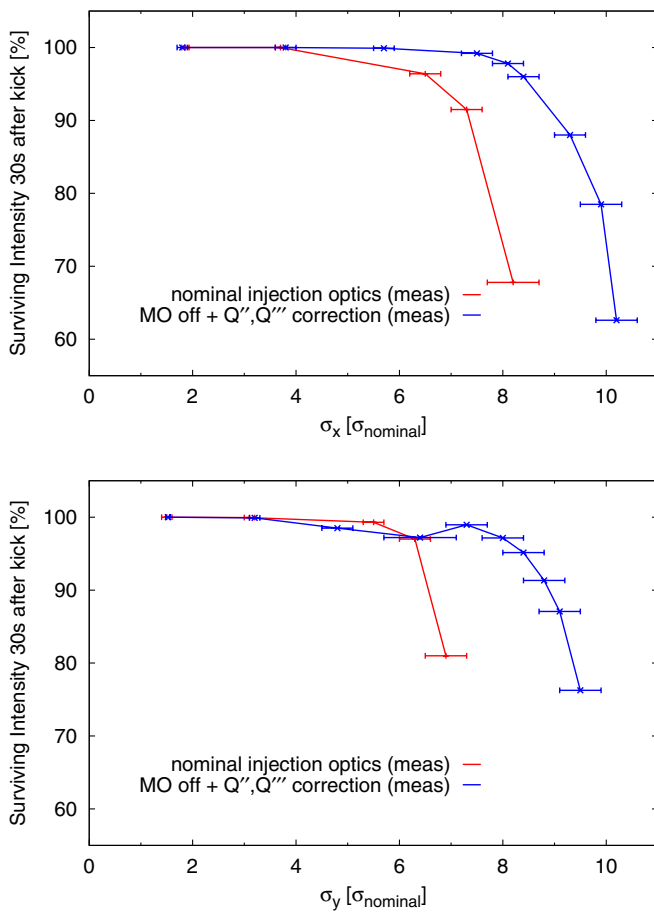
FIG. 13.   Surviving beam intensity versus horizontal (top) and vertical (bottom) kick amplitude in nominal sigma, 30 s after the kick was applied.

octupolar and decapolar nonlinearities (blue data in Fig. 13) the aperture was substantially increased. Consequently the aperture observed before correction at nominal injection optics (red data in Fig. 13) may confidently be identified with the dynamic aperture.

At the largest amplitudes considered by the DA measurement, imperfect correction of the BPM nonlinearity, as implemented in the LHC during 2012, caused a slight underestimate of the kick amplitude [21]. An improved correction method for BPM nonlinearity in the LHC has been developed for operation of the in 2015 [21]. To determine the dynamic aperture therefore, the BPM nonlinearity corrections applied online at the time of the measurement were inverted in the peak-to-peak data used to determine the kick amplitude (closed orbit was also taken into account), and the improved corrections applied. This increased the calculated kick amplitudes by $\sim 0.3\sigma_{\mathrm{nominal}}$ for the highest amplitude horizontal and vertical kicks, and by $0.5\sigma_{\mathrm{nominal}}$ for the highest amplitude diagonal kick.

The distance between the bunch center and the aperture was estimated in two ways. In the approximation of a Gaussian charge distribution, Eq. (12) was applied to the beam losses following those kicks which showed losses $\geq 20\%$. In most cases this was only the highest amplitude kick, however where more than one kick was used the results were very consistent (within $0.1\sigma_{\mathrm{nominal}}$). The beam loss due to a double Gaussian charge distribution, as measured by scraping the beams with collimators at injection in 2012 [26], was then compared with the measured loss curves of Fig. 13. The predicted loss curve fit very well to the observations, both at nominal injection settings and after correction of nonlinear sources. The aperture estimates agreed very well between the single and double Gaussian methods (within $0.1\sigma_{\mathrm{nominal}}$).

The amplitudes of the apertures corresponding to these measurements are given in Table V. The aperture was observed to increase following correction of octupolar and decapolar nonlinearities. The values before correction therefore, represent a measurement of the dynamic aperture of the LHC. The values after correction of octupolar and decapolar nonlinearities are harder to interpret. In the horizontal and vertical planes the aperture after correction increased to within $\sim 1.1\sigma_{\mathrm{nominal}}$ of the applied collimator aperture ($11.6\sigma_{\mathrm{nominal}}$). Furthermore the collimator

TABLE V.   LHC aperture determined from beam losses and turn-by-turn betatron oscillation data.

Angle	measurement $\pm$ error	
$\arctan\left(N_{\sigma y}/N_{\sigma x}\right)$	nominal optics	corrected optics
4°	$8.8 \pm 0.7\sigma_{\mathrm{nominal}}$	$10.8 \pm 0.6\sigma_{\mathrm{nominal}}$
40°	–	$11.1 \pm 0.6\sigma_{\mathrm{nominal}}$
80°	$8.8 \pm 0.6\sigma_{\mathrm{nominal}}$	$10.5 \pm 0.6\sigma_{\mathrm{nominal}}$

aperture is itself subject to uncertainties in relation to both the beta-beat and distortion of the closed orbit from the reference used to center the collimators about the beam. Losses on the collimators may therefore have contributed to the measured aperture in the horizontal and vertical planes.

Figure 14 plots the intensity of the LHC beams recorded by the beam current monitor (BCT) following the largest amplitude kicks in the horizontal, vertical, and diagonal planes at the corrected optics configuration. As described in Sec. II D losses against a physical aperture usually occur over a few turns. While the ~550 turn resolution of the

BCT does not allow for an absolutely conclusive determination of the source of the observed losses as the physical aperture, the abrupt drop in intensity observed for the horizontal and vertical kicks, followed by relatively flat losses is a very strong indication that for these kicks losses occurred on a physical limitation. In contrast the losses observed for the highest amplitude diagonal kick are characteristic of loss on the dynamic aperture.

The dynamic aperture in the model of nominal injection settings described in Sec. IV B 2 has been determined using SIXTRACK [36] for 3.3×10^5 turns. The simulation examined 50 angles in the (σ_x, σ_y) plane, tracking sets of 30 particles distributed in 2σ steps. Matching of the coupling was performed as described in Sec. IV B 2. Simulations with $|C^-| = 0.002$ and $|C^-| = 0.004$ were considered, corresponding to the uncertainty arising from local variations of $|f_{1001}|$. Four phases (0.0π, 0.5π, 1.0π and 1.5π) of f_{1001} at the matching point were considered for each amplitude examined. The WISE seeds of magnetic errors are included automatically by SIXTRACK. A comparison of the SIXTRACK simulation to the measured dynamic aperture is shown in Fig. 15. The phase and amplitude of f_{1001} is seen to have a notable impact upon the simulated dynamic aperture.

FIG. 14. Beam intensity recorded by the LHC Beam Current Monitors following the highest amplitude kicks performed in the horizontal, vertical, and diagonal planes at the corrected optics configuration.
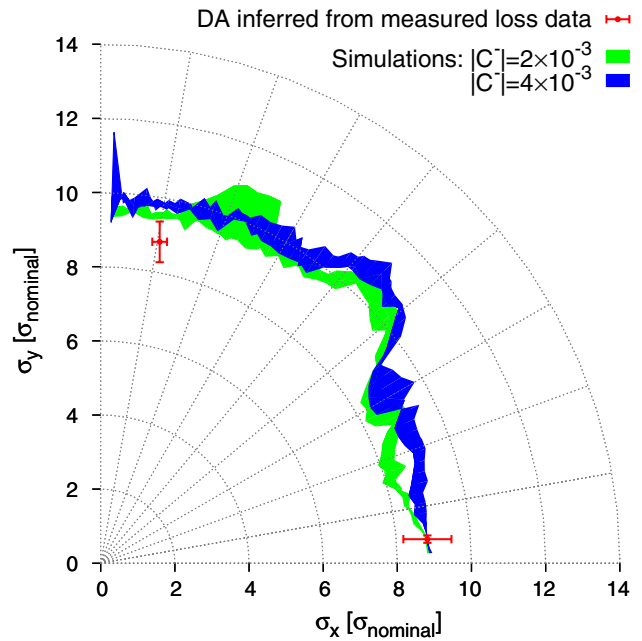

FIG. 15. Comparison of the modeled and measured dynamic aperture at nominal injection optics in the LHC. Simulations with $|C^-| = 0.002$ and $|C^-| = 0.004$ have been considered in order to characterize the uncertainty in the DA arising from the reproduction of $|f_{1001}|$ in the model. Similarly, four phases (0.0π, 0.5π, 1.0π and 1.5π) of f_{1001} at the matching point were considered for each amplitude examined. The area shown for the simulated amplitudes corresponds to the maximum and minimum DA defined by the four phases.
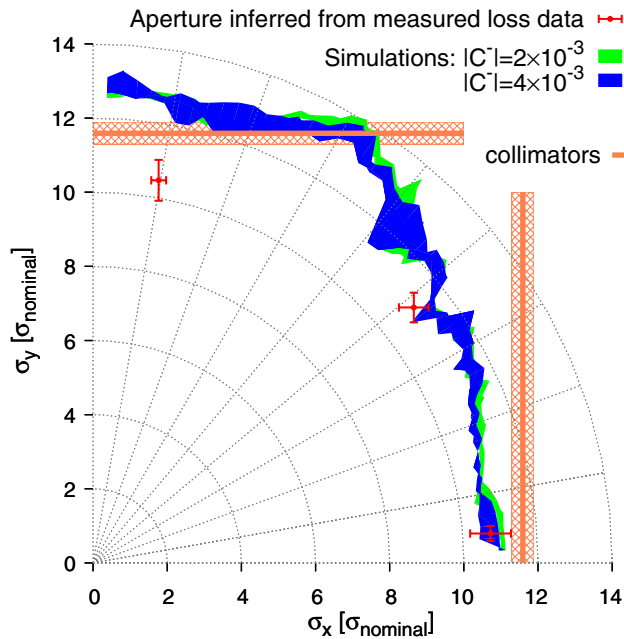
FIG. 16. Comparison of the modeled and measured dynamic aperture, following depowering of the MO and the application of corrections for Q'' and Q'''. Simulations with $|C^-| = 0.002$ and $|C^-| = 0.004$ have been considered in order to characterize the uncertainty in the DA arising from the reproduction of $|f_{1001}|$ in the model. Similarly, four phases (0.0π, 0.5π, 1.0π, and 1.5π) of f_{1001} at the matching point were considered for each amplitude examined. The area shown for the simulated amplitudes corresponds to the maximum and minimum DA defined by the four phases. Collimator settings are indicated by orange lines, where the patterned orange area indicates the uncertainty in collimator aperture defined by an assumed maximum beta-beat of 5%.

The agreement between model and measurement is very good. The measured DA in both planes agrees well inside the factor of two margin of safety ($DA_{\text{designed}}/DA_{\text{desired}} = 2$) which was specified during the LHC design phase. It is clear that to some degree the modeling of linear coupling is limiting the simulation of the nonlinear dynamics, up to the level of $\sim 1.5\sigma_{\text{nominal}}$ at certain angles. An improved method of local matching to the real f_{1001} in the machine may assist in this regard.

As described in Sec. IV B 2, a MAD-X model of the corrected optics was created by matching to the measured first order detuning. Following the matching of the first order terms, the second order detuning showed a similar qualitative behavior to the observations, but showed a $\sim 50\%$ deficit compared to the measured values. Dynamic aperture studies were performed on this model using SIXTRACK, the results are shown in Fig. 16. In Fig. 16 the settings of the collimators in the horizontal and vertical planes are indicated by solid orange lines. The aperture defined by the collimators in units of σ_{nominal} can be influenced by beta-beating at their location. An estimate of $\pm 0.3\sigma_{\text{nominal}}$ is obtained for the uncertainty collimator aperture, assuming a maximum beta-beat of 5%. This is

indicated in Fig. 16 by a patterned orange area about the collimator setting. Any distortion of the closed orbit from the reference used to center the collimators will also reduce the aperture. It has not been possible to quantify this effect, and no attempt is made to account for it in Fig. 16, however some departure from the reference should be expected due to the low intensity of the beams used for the DA measurement.

The simulated DA of the effective model showed an increase relative to that of the nominal machine, reflecting the observed increase in the real machine. The influence of the linear coupling on the dynamic aperture also appeared to be reduced upon reduction of the nonlinearities. At $\sim 11\sigma$, the simulated dynamic aperture agrees well with the measured value for the diagonal kicks. In the horizontal plane it is difficult do draw meaningful conclusions: the measured aperture, simulated DA, and collimator aperture (which it should be noted does not include reduction due to closed orbit distortion away from the reference orbit) are all approximately consistent. In the vertical plane detailed conclusions regarding the validity of the matched model cannot be drawn beyond the fact that the vertical dynamic aperture is outside the aperture of the collimators, as appeared to be the case in the real machine.

V. CONCLUSIONS

Measurements of several nonlinear observables have been performed in the LHC using kicked beams. The results have been compared to simulation allowing us to assess the understanding of the nonlinear transverse dynamics of the machine.

The detuning with amplitude of the accelerator was measured at nominal injection optics. It was found that first order amplitude detuning was large, but agreed well with the modeled values. Second order amplitude detuning was also measured in the LHC for the first time. While the simulated second order detunings showed a qualitatively similar behavior to the measurements, there were significant deficits. At the highest amplitudes examined this resulted in a delayed approach of the model to the third and fourth order resonances. These discrepancies are smaller, but still relevant, within the aperture defined by the collimators in operation. Further studies will be required to improve the understanding of these higher order effects. Following measurements at nominal injection optics, Landau octupoles were depowered and corrections for the nonlinear chromaticities (found in 2011) were applied. Significant reductions in the amplitude detuning were observed, which led to improved decoherence of kicked beams.

During measurements of the detuning with vertical amplitude performed at nominal injection optics, a substantial coupling of the large amplitude vertical kicks into the horizontal plane was observed. This corresponded with the tune split approaching a δQ_{min} which was considerably in excess of the linear $|C^-|$. It has been concluded that an amplitude dependent nonlinear coupling was observed.

The approach to the $\delta Q_{\min}$ and the coupling of vertical kicks into the horizontal plane are reproduced in the model, representing a further verification of the understanding of the nonlinear dynamics in the LHC.

The dynamic aperture at nominal injection optics was measured. Agreement with the model was good in both planes, particularly in the horizontal. The measured and simulated dynamic aperture agreed well within the safety margin specified in the LHC design phase. It was shown that through a minimization of readily observed nonlinear parameters it is possible to increase the dynamic aperture in the LHC.

These observations validate many aspects of the LHC nonlinear model at nominal injection optics, in particular: the first order detuning, the nonlinear coupling, and the dynamic aperture. Some areas have been highlighted as requiring further study however, notably the higher order terms in the amplitude detuning, and the requirement for a better linear coupling model. Observation of the nonlinear coupling, and its reproduction in the model, have opened the door to more detailed studies of this phenomenon. The ability to control the nonlinear transverse dynamics has been well established by the manipulations performed during this experiment. Most notably the demonstration of dynamic aperture correction in the LHC is an important step forward. These are promising results for the future exploitation of the LHC.

ACKNOWLEDGMENTS

[1] M. Aiba, S. Fartoukh, A. Franchi, M. Giovannozzi, V. Kain, M. Lamont, R. Tomás, G. Vanbavinckhove, J. Wenninger, F. Zimmermann, R. Calaga, and A. Morita, Phys. Rev. ST Accel. Beams **12**, 081002 (2009).

[2] R. Tomás, O. Bruning, M. Giovannozzi, P. Hagen, M. Lamont, F. Schmidt, G. Vanbavinckhove, M. Aiba, R. Calaga, and R. Miyamoto, Phys. Rev. ST Accel. Beams **13**, 121004 (2010).

[3] C. Alabau Pons, E. H. Maclean, F. Schmidt, and R. Tomás, Report No. CERN-ATS-Note-2011-096 TECH, 2011.

[4] C. Alabau Pons, E. H. Maclean, F. Schmidt, and R. Tomás, in *Proceedings of the 2nd International Particle Accelerator Conference, San Sebastián, Spain* (EPS-AG, Spain, 2011), p. WEPCO79.

[5] R. Tomás, R. Calaga, A. Langner, Y. I. Levinsen, E. H. Maclean, T. H. B. Persson, P. K. Skowronski, M. Stzelczyk, G. Vanbavinckhove, and R. Miyamoto, Phys. Rev. ST Accel. Beams **15**, 091001 (2012).

[6] T. H. B. Persson, Y. I. Levinsen, R. Tomás, and E. H. Maclean, Phys. Rev. ST Accel. Beams **16**, 081003 (2013).

[7] M. Albert, G. Crockford, S. Fartoukh, M. Giovannozzi, E. H. Maclean, A. MacPherson, R. Miyamoto, L. Ponce, S. Redaelli, F. Roncarolo, F. Schmidt, R. Steinhagen, E. Todesco, R. Tomás, G. Vanbavinckhove, and W. Venturini Delsolaro, Report No. CERN-ATS-Note-2011-052 MD, 2011.

[8] E. H. Maclean, F. Schmidt, R. Tomás, R. Bartolini, E. Todesco, R. Steinhagen, G. Vanbavinckhove, and M. Giovannozzi, in *Proceedings of the 2nd International Particle Accelerator Conference, San Sebastián, Spain* (EPS-AG, Spain, 2011), p. WEPCO78.

[9] G. Vanbavinckhove, M. Aiba, R. Bartolini, R. Calaga, M. Giovannozzi, E. H. Maclean, R. Miyamoto, F. Schmidt, and R. Tomás, in *Proceedings of the 2nd International Particle Accelerator Conference, San Sebastián, Spain* (EPS-AG, Spain, 2011), p. WEPCO32.

[10] E. H. Maclean, S. Moeckel, T. H. B. Persson, S. Redaelli, F. Schmidt, R. Tomás, and J. Uythoven, Report No. CERN-ATS-Note-2013-022 MD, 2013.

[11] M. Albert, G. Crockford, S. Fartoukh, M. Giovannozzi, E. H. Maclean, A. MacPherson, R. Miyamoto, L. Ponce, S. Redaelli, H. Renshall, F. Roncarolo, R. Steinhagen, E. Todesco, R. Tomás, and W. Venturini Delsolaro, in *Proceedings of the 3rd International Particle Accelerator Conference, New Orleans, LA, 2012* (IEEE, Piscataway, NJ, 2012), p. TUPPCO81.

[12] S. Cettour Cave, R. De Maria, M. Giovannozzi, M. Ludwig, A. MacPherson, S. Redaelli, F. Roncarolo, M. Solfaroli Camillocci, and W. Venturini Delsolaro, Report No. CERN-BE-2013-002 MD, 2013.

[13] R. Jones, Report No. CERN-BE-2010-007, 2010.

[14] A. Bazanni, E. Todesco, and G. Turchetti, Report No. CERN 94-02, **94**, 02.

[15] R. A. Barlow, E. Carlier, J. P. Pianfetti, V. Senaj, and M. Cattin, Report No. CERN-TE-Note-2010-001.

[16] E. Carlier, L. Ducimetiere, E. Vossenberg, in *Conference Record of the Twenty Seventh International Power Modulator Symposium* (IEEE, Arlington, VA, 2006).

[17] J. Uythoven, Report No. CERN TE-ABT-BTP; (private communication).

[18] R. Bartolini and F. Schmidt, Report No. CERN SL/Note 98-017 (AP), 2010.

[19] A. Sherman, Report No. CERN-STUDENTS-Note-2013-215.

[20] C. Boccard, E. Calvo, L. Jensen, R. Jones, T. Lefevre, A. Margiolakis, and A. Nosych, in *LHC OMC Review, 17 June 2013.*

[21] A. Nosych, LHC Report No. 1342295.

[22] R. Calaga and R. Tomás, Phys. Rev. ST Accel. Beams **7,** 042801 (2004).

[23] S. White, E. Maclean, and R. Tomás, Phys. Rev. ST Accel. Beams **16,** 071002 (2013).

[24] M. G. Minty and F. Zimmermann, Report No. SLAC-R-621, 2003, http://www.slac.stanford.edu/cgi-wrap/getdoc/slac-r-621.pdf.

[25] A. Boccardi, M. Gasior, O. R. Jones, P. Karlsson, and R. J. Steinhagen, Report No. CERN-LHC-Performance-Note-007, 2013.

[26] L. Drosdal, K. Cornelis, B. Goddard, V. Kain, M. Meddahi, O. Mete, B. Salvachua, G. Valentino, and E. Veyrunes, in *Proceedings of the 4th International Particle Accelerator Conference, IPAC-2013, Shanghai, China, 2013* (JACoW, Shanghai, China, 2013), p. MOPWO032.

[27] http://mad.web.cern.ch/mad/.

[28] WISE homepage, http://wise.web.cern.ch/WISE/.

[29] WISE geometry page, http://wise.web.cern.ch/WISE/Other/Geometry/.

[30] P. Hagen, WISE - user guide and implementation notes, http://wise.web.cern.ch/WISE/Doc/lhc-project-report-wise.pdf.

[31] E. Todesco (private communication).

[32] E. H. Maclean, in *LHC OMC Review (2013).*

[33] A. Franchi, Ph.D. thesis, Universita FrankfurtU, 2006; http://www.gsi.de/en/start/beschleuniger/fachabteilungen/accelerator_physics/phd_thesis.htm.

[34] R. Tomás, Report No. CERN-ATS-Note-2012-019 MD, 2012.

[35] É. Forest, F. Schmidt, and E. McIntosh, Report No. CERN-SL-2002-044 (AP), 2002.

[36] SixTrack - 6D Tracking Code, http://sixtrack-ng.web.cern.ch/sixtrack-ng/.

[37] R. Jones, P. Cameron, and Y. Luo, Report No. C-A/AP/#204, 2005.